Title: **Using the right side of Poisson's equation to save on numerical calculations in FEM simulation of electrochemical systems**
Author(s): Montoya R.; Galvan J. C.; Genesca J.
Source: CORROSION SCIENCE Volume: **53** Issue: **5** Pages: **1806-1812**
DOI: **10.1016/j.corsci.2011.01.059** Published: **MAY 2011**

Graphical Abstract:

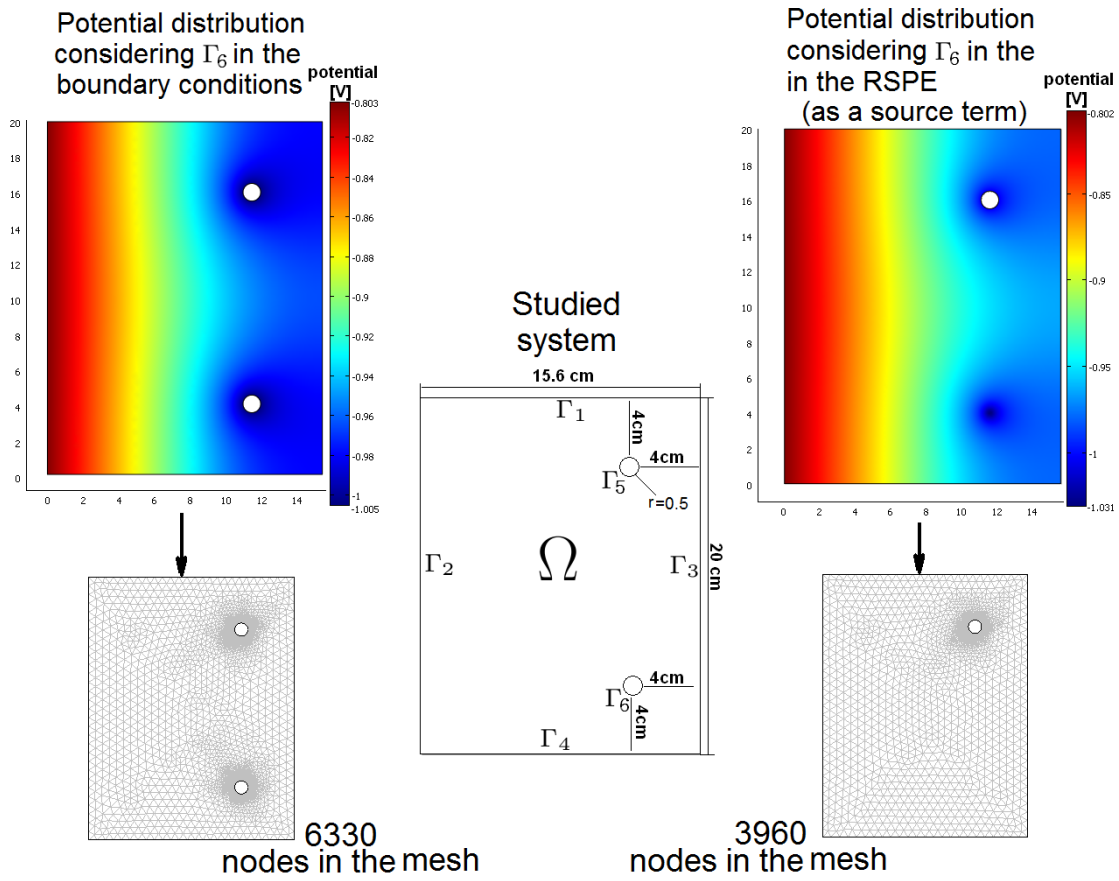

Research highlights

► The equivalence between RSPE and the constant potential electrodes was verified. ► For 2D circular electrodes their mathematical relationship is provided. ► It is possible to use electric sources as constant potential regions and vice versa. ► Considering constant potential regions as the source term the domain remains always the same. ► The above leads to save calculations in modeling electrochemical systems with FEM.

Article title: Using the right side of Poisson's equation to saveon numerical calculations in FEM simulation ofelectrochemical systems

Authors: R. Montoya [a,b,c,1], J.C. Galván[a,1], J. Genesca[c]

Affiliations:

[a]Centro Nacional de Investigaciones Metalúrgicas (CENIM), CSIC Avda. Gregorio del Amo, 8,28040 Madrid, Spain

[b]Departamento de Matemáticas, Facultad de Química, Universidad Nacional Autónoma de México, UNAM, Ciudad Universitaria, 04510 México D.F. (Mexico)

[c]Dept. de Ingeniería Metalúrgica, Facultad de Química, Universidad Nacional Autónoma de México, UNAM, Ciudad Universitaria, 04510 México D.F. (Mexico)

Abstract

This work justifies using the right side of Poisson's equation (RSPE)[2] to simulate constant potential electrodes (CPEl) in electrochemical processes. Thesehave traditionally been considered in the boundary conditions of the corresponding boundary value problem (BVP), but in some cases working with the RSPEis much more versatile, efficient and suitable. If constant potential regions areconsidered as boundaries, then the domain constantly changes as the number,size and position of the regions change; but if they are considered as the sourceterm, the domain remains the same, no matter how many electrodes there are orhow or where they are located. Some examples will be solved in order to clearlyshow that the complicated process of redefining a domain

---

[1]Corresponding authors: Tel:+34915538900. FAX:+34915538900
e-mail addresses: rodrigo.montoya@cenim.csic.es, jcgalvan@cenim.csic.es
[2]Also called source terms.

mesh and numbering its corresponding nodes in the finite element method (FEM) is sometimesunnecessary when the electrodes are represented with a suitable function on theRSPE. These practical examples are simulated using a finite element programdeveloped by the authors.

Keywords:

A. Mild steel

B. Modelling studies

B. Polarization

C. Cathodic protection

Introduction

As is known, minimization costs and maximization of the efficiency in engineering processes are imperative in the competitive electrochemical and anticorrosive industry. In this sense the mathematical modeling is a powerful tool; therefore minimization of response times in computational codes becomes essential.

To date, a great number of articles have been published, mainly concerned to cathodic protection, which numerically solve the Poisson's equation in order to predict the distribution of electrochemical potentials in a domain of interest [1-17]. In all these works, CPEl are usually considered in boundary conditions and the RSPE as zero, although it is known that the RSPE can be used to represent polarization current densities [5].

In this work CPEl will be considered as sites with a continuous charge distribution on the RSPE, a clear relation between this and the constant potential regions will be verified, and in the case of 2D circular CPEl the explicit mathematical relation will be provide.

The ideas developed in this work are useful not only for saving a huge quantity

of numerical calculations in modeling electrochemical systems with FEM, e.g. Lithium-ion batteries, fuel cells, supercapacitors, cathodic protection, corrosion processes, etc. but also, where appropriate and depending on the circumstances, to treat electric sources as constant potential regions and vice versa.

In order to simplify the work of plotting the solutions it was decided to write the code in the commercial, and well known, Canadian software Maple® using its particular programming language.

We presume any commercial finite element program must build the same answer if the same parameters are introduced. Recently we have verified the responses by using the commercial software COMSOL® and the results have been exactly the same.

The case of a CPEl in an insulated system, a trivial case

To find the potential distribution at equilibrium in the case shown in Figure 1(a) it is necessary to solve, if possible, BVP 1, which considers the CPEl as aboundary and is posed below,

$$-k\Delta\phi(x,y) = 0 \quad (x,y)\epsilon\Omega \qquad (1)$$

$$-k\frac{\partial\phi}{\partial n} = 0 \text{ in}\Gamma_1 \cup \Gamma_2 \cup \Gamma_3 \cup \Gamma_4$$

$$\phi = \phi_0 \text{in}\Gamma_5$$

Where ϕ is the electrochemical potential indomainΩ, k represents the electrolyte conductivity and ϕ_0 is the fixed potential of anode Γ_5.Γ_1, Γ_2, Γ_3 and $\Gamma_4$represent electrically insulated boundaries.

Problem 1 presents both Neumann and Dirichlet type boundary conditions, which together with the operator used (Laplacian) make for a problem with a unique solution, since its corresponding weak formulation $a(\cdot, \cdot) = l(\cdot)$ has a left side that is bilinear,

symmetrical, continuous and H-elliptic, while the function $l(\cdot)$ is linear and continuous [18, 19].

In order to solve problem 1, first of all the corresponding variational formulation is generated. This is posed in a space of finite dimension and the finite element method is ultimately applied in order to solve the numerical system obtained.

For more detailed information on the procedure applied, see Appendix I.

Physical analysis of the situation shown in Figure 1 (a), the boundary conditions used in problem 1 and the last matricial system in Appendix I clearly reveal that the solution to this trivial system is $\phi_0 \text{in}\Omega$, because it is an electrically insulated domain with only a portion of the boundary subject to a constantpotential ϕ_0, and thus at equilibrium the domain takes this potential.

The case of an anode and a cathode in a system with insulated boundaries

If boundary Γ_2 in Figure 1(a) is subjected to a current flow denominated PC, which is a function that represents the cathodic polarization curve of a metal *M*; the rest of the external boundaries remain electrically insulated and the circular boundary maintains the potential ϕ_0, which is anodic with respect to metal *M*, then the case would represent a cathodic protection system and its corresponding BVP is as follows,

$$-k\Delta\phi(x,y) = 0 \quad (x,y)\epsilon\Omega \qquad (2)$$

$$-k\frac{\partial\phi}{\partial n} = 0 \text{ in}\Gamma_1 \text{U}\Gamma_3 \text{U}\Gamma_4$$

$$-k\frac{\partial\phi}{\partial n} = PC\text{in}\Gamma_2 \text{and}\phi = \phi_0 \text{in}\Gamma_5$$

thevariational formulation and the matricial posing of this problem are obtained in a similar way to problem 1, with the difference that the new Neumann condition in Γ_2 is

not considered to define the variation space V because this is not denominated an essential boundary condition [18, 19].

The final matricial form of the new problem in question would be:

$$\begin{bmatrix} \int_\Omega \frac{\partial \Phi_1}{\partial x}\frac{\partial \Phi_1}{\partial x} + \frac{\partial \Phi_1}{\partial y}\frac{\partial \Phi_1}{\partial y} dX & \dots & \int_\Omega \frac{\partial \Phi_N}{\partial x}\frac{\partial \Phi_1}{\partial x} + \frac{\partial \Phi_N}{\partial y}\frac{\partial \Phi_1}{\partial y} dX \\ \vdots & \ddots & \vdots \\ \int_\Omega \frac{\partial \Phi_1}{\partial x}\frac{\partial \Phi_N}{\partial x} + \frac{\partial \Phi_1}{\partial y}\frac{\partial \Phi_N}{\partial y} dX & \dots & \int_\Omega \frac{\partial \Phi_N}{\partial x}\frac{\partial \Phi_N}{\partial x} + \frac{\partial \Phi_N}{\partial y}\frac{\partial \Phi_N}{\partial y} dX \end{bmatrix} \begin{bmatrix} a_1 \\ \vdots \\ a_N \end{bmatrix}$$

$$= \begin{bmatrix} \int_{\Gamma_2} PC\Phi_1 \\ \vdots \\ \int_{\Gamma_2} PC\Phi_N \end{bmatrix} \quad (3)$$

So it only remains to find the unknown vector $\{a_1,\dots,a_N\}$ using a numerical method. The BVP of problem 2 would be different if it had been decided to consider the constant potential condition ϕ_0 for Γ_5 on the RSPE and not in the boundary conditions. In this case the corresponding BVP would be,

$$-k\Delta\phi(x,y) = f(x,y)(x,y)\epsilon\Omega \quad (4)$$

$$-k\frac{\partial \phi}{\partial n} = 0 \text{ in}\Gamma_1 \cup \Gamma_3 \cup \Gamma_4$$

$$-k\frac{\partial \phi}{\partial n} = PC\text{in}\Gamma_2$$

Where *f(x, y)* is the RSPE where the circular electrode is considered. However, this problem only has Neumann type conditions, and according to the functional analysis theory there is no unique solution [18, 19, 4] and there is no sense to search for its physical solution. Figure 1 (b) graphically shows the numerical response obtained by

FEM in problem 2. This is done by making ϕ_0 = -1005 mV, k = 4 S/mand $-k\frac{\partial \phi}{\partial n}$ = PC_{xjia}A/m^2, wherePC_{xjia} is the function that represents the cathodic polarization curve of mild steel in 5% NaCl solution reported in [17].

The case of one cathode and two or more anodes in a system with insulated boundaries

In both corrosion engineering and electrochemical science there are a number of situations in which testing must be performed with more than one anode and different anode positions e.g. the case of potential optimisation in a particular domain region. As a consequence, thedomain Ωmesh is enormously complicated because it depends not only on the number of selected elements in the domain but also on the system's geometry, which changes according to the selected anode position and with the addition of each new anode.

If the physical problem facing us on this occasion is that represented in Figure 2(a), then the corresponding BVP would be very similar to problem (2), except that the new system requires an additional boundary.

However, in this problem one of the anodes may be considered on the RSPE, because in this way the corresponding BVP would use both Dirichlet and Neumann conditions, thus avoiding the need to satisfy the inadequate compatibility condition [18, 19] required to guarantee the existence of a solution in problems that consider only Neumann conditions. Thus, the problem in Figure 2(a) may be mathematically represented and solved according to BVP 5 or 6 presented below.

If the two anodes shown in Figure 2(a) are considered as boundaries, then their corresponding BVP is,

$$-k\Delta\phi(x,y) = 0 \quad (x,y)\epsilon\Omega \qquad (5)$$

$$-k\frac{\partial\phi}{\partial n} = 0 \text{ in}\Gamma_1 \cup \Gamma_3 \cup \Gamma_4$$

$$-k\frac{\partial\phi}{\partial n} = PC \text{in}\Gamma_2 \text{and}\phi = \phi_0 \text{in}\Gamma_5 \cup \Gamma_6$$

Whereas, in contrast, if the condition in Γ_6 is considered on the RSPE, the corresponding BVP is,

$$-k\Delta\phi(x,y) = f(x,y) \quad (x,y)\epsilon\Omega \tag{6}$$

$$-k\frac{\partial\phi}{\partial n} = 0 \text{ in}\Gamma_1 \cup \Gamma_3 \cup \Gamma_4$$

$$-k\frac{\partial\phi}{\partial n} = PC \text{in}\Gamma_2 \text{and}\phi = \phi_0 \text{in}\Gamma_5$$

It should be mentioned that in this last case the Γ_6 boundary does not exist and the condition of this place being at a certain potential is approximated by $f(x, y) = r\ exp\{(-s(x - x_0)^2 - s(y - y_0)^2\}$[3], where *r* is a factor that involves the potential or the current at which the electrode is found, *s* is a proportionality factor of the electrode diameter, and x_0 and y_0 are the coordinates of the center of the electrode [15, 16].

We are now in a position to solve either of the two above problems to find the potential distribution of the case shown in Figure 2(a). Problem 6 may be solved with the same mesh used in problem 2, while problem 5 needs a new mesh and will need a different one for each new anode position.

Results and discussion

Figures 2(b) and 2(c) show the solution to problems 5 and 6, respectively, revealing very similar symmetrical potential distributions around the mid horizontal axis of the

[3] More about the determination of this function can be seen in the Appendix II.

figure. The main difference between the two figures is that Figure 2(c) shows the solution in the lower anode while Figure 2 (b) does not; since this region does not belong to domain Ω because the anode is considered as a boundary in the corresponding BVP. This is what causes the different color scale in the two figures, since the centre of the lower anode in case (b) is more negative and thus needs a greater resolution. However, the potential values are very similar in the rest of the domain, which demonstrates that the $f(x, y)$ proposed in [15] and [16] to represent circular CPEl on the RSPE is correct and responds almost identically to the corresponding simulation of circular anodes in the boundary conditions.

Figure 5 shows, in a quantitative way, the profile of the electrochemical potential of the four paths selected from Figure 2 (a). With these results it becomes clearer the real equivalency existent between problem (6) and problem (5) using $f(x,y)$ suggested here.

Similarly, another anode may be added to the system without the need to alter the mesh in the preceding problem. In this case it is only necessary to modify $f(x, y)$ by adding a term. Specifically, to represent the anode configuration shown in Figure 3(a), $f(x,y)$ was considered as $r_0(exp\{(-s(x -x_0)^2- s(y-y_0)^2\})+r_1exp\{-s(x-x_1)^2-s(y-y_1)^2\})$ where (x_1,y_1) are the coordinates of the centre of the third anode, so the BVP of the case shown in Figure 3(a) is identical to problem 5 except for the term $r(exp(-s(x-x_1)^2-s(y-y_1)^2))$ involved in function $f(x, y)$. The numerical response of this example is represented in Figure 3(b). The similarity of the potential distribution in Figures 3(b) and 3(c) reveals that the anodes have the same response when considered either in $f(x,y)$ or in boundary conditions.Similar profiles to Figure 5 are obtained in this case. It means, almost identical potentials profiles are obtained, in all paths tested, when the three anodes are considered as boundaries and when two of them are considered in $f(x,y)$.

It is evident that in the two above examples and in all those where the RSPE is considered, the computational code that is used must solve extra numerical integrals that involve *f(x,y)*. However, modern numerical integration methods, such as the well-known quadrature method, place greater emphasis on avoiding the numbering and renumbering relationship of the meshing process before writing an integration algorithm.

Figure 4 shows quantitatively the numerical calculations saving when the RSPE is employed instead of two and three circular boundary conditions. In all cases coarse (A), medium (B) and fine (C) grids were used. It is important to keep in mind that Figure 4 *(I-C)* is the mesh used to obtain not only Figure 1(b) but also 2(c) and 3(c).

When a coarse mesh is employed there is a difference of almost 600 elements between the numerical systems used in problems 6 and 5, and this number increases until almost 9500 with a fine meshing. Both quantities increase twice when a third circular electrode is considered. In other words, the corresponding square matrix (called stiffness matrix) used to obtained the answer showed in Figure 3(c) has a size 15840×15840 while the size of the matrix used to obtain the solution of Figure 3(b) is 34336x34336.

Talking about numerical calculation savings in terms of nodes in the selected mesh is a quantitative way to measure a saving, because others variables like time response depends mainly on different factors like the software, the computer and often on the users' skills. For example: using the software developed in this work, the response times , in order to obtain the results showed in Figures 2 b), 2 c), 3 b) and 3 c), were 19´42´´, 11´54´´, 42´10´´, 12´39´´ respectively. However, when using the commercial software COMSOL®, the response times for these four cases are almost the same and there are no differences > 5 seconds. On the other hand, starting with the same domain showed in Figure 1 a) the time wasted to "redraw" a new domain to obtain the responses showed

in Figures 2 b) and 3 b) could be, depending of the user' skills, from 1 hour to, even, several hours using the code built by the authors and up to half an hour in the case of the commercial program. While in the case of Figures 2 c) and 3 c) the user will spend no more than a few seconds, in both programs, modifying *f(x,y)* from its initial value, zero, used to obtained the response showed in Figure 1 b).

Conclusions

The validity of using the RSPE has been demonstrated by finding that, if adequate parameters are considered, the solution of a BVP containing two or more constant potential electrodes in boundary conditions is almost identical to the solution of the corresponding BVP considering the RSPE. Furthermore, the need to work with different meshes when taking into consideration different CPEl positions is avoided, so once the corresponding domain has been meshed, any number of different positions may be used without the need to redefine a new mesh. However, it should be kept in mind, that mathematical theory makes it necessary to consider at least one Dirichlet type condition in order to be able to represent these regions on the RSPE.

It has been demonstrated that saving in numerical computations, when the RSPE is used, is achieved not only increasing the number of CPEl but also when a refining meshing is made.

It has also been verified that the equation *f(x, y),* proposed in [15] to represent circular CPEl in 2D on the RSPE, is fully suitable; not only because of the adequate potential

values that are obtained but also because of its versatility and efficiency in representing a system with multiple electrodes of different sizes, positions and potentials.

Using this function offers countless advantages as the number, size or difference in potential between the anodes represented increases, since for *n* anodes *f(x, y)* is simply expressed in the form *of* $r_0(exp\{(-s_0(x-x_0)^2 - s_0(y-y_0)^2\}) + \ldots + r_{n-1}(exp\{(s_{n-1}(x-x_{n-1})^2 - s_{n-1}(y-y_{n-1})^2\})$ without interfering at all with the meshing of the problem provided that the mesh is sufficiently fine.

In summary, the equivalence between the RSPE [A/m^3] and the CPEl [V] has been verified and in the case of 2D circular CPEl their explicit mathematical relationship is provided.

Appendix I

Before going on with the variational formulation of problem 1 it is necessary tohomogenise the Dirichlet type boundary condition and redefine the problem as follows,

$$-k\Delta\phi(x,y) = 0 \quad (x,y)\epsilon\Omega \tag{7}$$

$$-k\frac{\varphi\phi}{\partial n} = 0 \text{ in}\Gamma_1 \cup \Gamma_2 \cup \Gamma_3 \cup \Gamma_4$$

$$\phi = 0 \text{ in}\Gamma_5 \tag{4}$$

Subsequently the variational space ν is defined with the essential boundary conditions [18, 19] of problem 7:

$$\mathcal{V} = \{v \in H^1(\Omega) : v(\Gamma_5) = 0\}$$

---

[4]To achieve this homogenization it is necessary to make a simple change of variable and use another change, at the end of the process, in the reverse direction in order to recover the original solution of the physical problem.

where$H^m(\Omega) = \{v : \partial_\alpha v \in L^2(\Omega) \forall \alpha \ni |\alpha| < m\}$and

$L^2(\Omega) = \left\{f: \Omega \to \mathbb{R} | \int_\Omega |f(x)|^2 \, dx < \infty\right\}$[5], when each member of equation 7 is multiplied by *v* and is integrated in domain Ω, we obtain:$\int_\Omega kv\Delta\phi = -\int_\Omega fv \forall v \in \mathcal{V}$, to which Green's theorem is applied to obtain the following equation:

$\int_\Omega div(v\nabla\phi)dx - \int_\Omega \nabla\phi \cdot \nabla v dx = -1/k \int_\Omega fv \forall v \in \mathcal{V}$,

and using the divergence theorem the latter is transformed into

$\int_{\Gamma_1 U \Gamma_2 U \Gamma_3 U \Gamma_4 U \Gamma_5} v\nabla\phi \cdot n - \int_\Omega \nabla\phi \cdot \nabla v dx = -1/k \int_\Omega fv \forall v \in \mathcal{V}$.

Finally, the boundary conditions are used and it is considered that in this particular case *f(x, y)* = 0 to obtain

$$\int_\Omega \nabla\phi \cdot \nabla v = 0 \, \forall v \in \mathcal{V} \qquad (8)$$

Before applying FEM it is necessary to address problem 8 in a space of finitedimension, for which a partition of Ω is fixed with N parts and a subspace of νis considered with a finite dimension referred to as C_N. This will be formed byfunctions

$\varphi: \Omega \to \mathbb{R}$

such as:

- $\varphi_i$is continuous
- φ_i is a polynomial in $\mathbb{R}^2$ *for i= 1, … , N*

Now the problem is to find $\phi_N \in C_N$, so that

$$\int_\Omega \nabla\phi \cdot \nabla v = 0 \, \forall v \in \mathcal{V}$$

LetΦ_i, *i = 1..N* a base of C_N. Then the solution ϕ_N must be a linear combination of Φ_I, so

---

[5]This integral is used in the Lebesgue sense.

$$\phi_N = \sum_{i=1}^{N} a_i \Phi_i$$

Where the coefficients a_i are converted into the unknown vectors. In this way the problem is reduced to

$$\sum_{i=1}^{N} a_i \int_\Omega \left(\frac{\partial \Phi_i}{\partial x}(x,y), \frac{\partial \Phi_i}{\partial x}(x,y) \right) \cdot \nabla v(x,y) dA = 0$$

in particular, if *v* is considered as a base element Φ_i, then:

$$\sum_{i=1}^{N} a_i \int_\Omega \left(\frac{\partial \Phi_i}{\partial x}(x,y), \frac{\partial \Phi_i}{\partial x}(x,y) \right) \cdot \left(\frac{\partial \Phi_j}{\partial x}(x,y), \frac{\partial \Phi_j}{\partial x}(x,y) \right) dA = 0;\ j = 1, \dots, N$$

or in matricial form:

$$\begin{bmatrix} \int_\Omega \frac{\partial \Phi_1}{\partial x}\frac{\partial \Phi_1}{\partial x} + \frac{\partial \Phi_1}{\partial y}\frac{\partial \Phi_1}{\partial y} dX & \dots & \int_\Omega \frac{\partial \Phi_N}{\partial x}\frac{\partial \Phi_1}{\partial x} + \frac{\partial \Phi_N}{\partial y}\frac{\partial \Phi_1}{\partial y} dX \\ \vdots & \ddots & \vdots \\ \int_\Omega \frac{\partial \Phi_1}{\partial x}\frac{\partial \Phi_N}{\partial x} + \frac{\partial \Phi_1}{\partial y}\frac{\partial \Phi_N}{\partial y} dX & \dots & \int_\Omega \frac{\partial \Phi_N}{\partial x}\frac{\partial \Phi_N}{\partial x} + \frac{\partial \Phi_N}{\partial y}\frac{\partial \Phi_N}{\partial y} dX \end{bmatrix} \begin{bmatrix} a_1 \\ \vdots \\ a_N \end{bmatrix} = \begin{bmatrix} 0 \\ \vdots \\ 0 \end{bmatrix} \qquad (9)$$

The problem ends when a numerical algorithm is used to solve the above system. From the latter matricial system it follows that the solution is trivial, i.e.$\{a_1, \dots, a_N\} = \{0, \dots, 0\}$, and so when the variable is changed[6] the final solution is ϕ_0.

Appendix II

The source term *f(x,y)* was found by searching for a continuous function whose compact support was identical to the perimeter of the anode. In other words, a search was conducted to find a continuous function whose values outside of the circular anode were zero. Achieving this is really complicated, however, a good approximation of a function with circular compact support is $r\ exp\{(-s(x-x_0)^2 - s(y-y_0)^2\}$ because, as seen in Figure 6, outside of the 'protuberance' the function values are almost nil. Additionally,

[6]In order to recover the original solution of the physical problem and not that of the homogeneous problem.

the centre of this function - and the centre of its ‘protuberance’- is located exactly in coordinates (x_0,y_0), the diameter of the base of this ‘protuberance’ is inversely proportional to the parameter *S*- It means, the diameter of the anode is inversely proportional to this parameter- and finally, the height of the function is the parameter *r* and is related to the potential at which the anode is set.

Certainly, the determination of *r* depends not only on the potential at which the anode is set, but also on the geometry of the domain and on the localization of the (x_0,y_0). Although it is possible to determine *r* in every possible case, proper treatment of the problem must be made and it is not an easy task. However, for the cases studied in this paper we ensure *r* is -4.9 for the case showed in Figure 2 c) and -3.61 for the case of three anodes showed in Figure 3c). The value of *s* does not represent a problem and its value, in both cases, was considered as 19.7.

Acknowledgments

This work has been supported by the Ministry of Science and Innovation of Spain, MICINN (Projects MAT2006-04486 and MAT2009-13530). R.M. acknowledges a postdoctoral contract financed by National Autonomous University of Mexico, UNAM-DGAPA.

References

[1] R.D. Strømmen, Computer Modeling of Offshore Cathodic Protection Systems: Method and Experience, in: Computer Modeling in Corrosion, R.S. Munn, Editor, ASTM STP 1154, American Society for Testing and Materials, Philadelphia, PA (1992) pp. 229-247.

[2] J.C.F. Telles, W.J. Mansur, L.C. Wrobel, M.G. Marinho, Numericalsimulation of a cathodically protected semisubmersible platform using the PROCAT system, *Corrosion*, **46**, (1990) 513-518.

[3] S.L.D.C. Brasil, L.R.M. Miranda, J.C.F. Telles, A Boundary Element Study of Cathodic Protection Systems in High Resistivity Electrolytes, in: Proceedings of the NACE99 Topical Research Symposium: Cathodic Protection: Modeling and Experiment, M.E. Orazem, Editor, NACE International, Houston, TX (1999) pp.153-172.

[4] R.S. Munn, O.F. Devereux, Numerical modeling and solution of galvanic corrosion systems. Part 2 - Governing differential-equation and electrodic boundary-conditions, *Corrosion*, **47**, (1991) 618-632.

[5] R.S. Munn, A mathematical-model for a galvanic anode cathodic protection system, *Mater. Perform.*,**21**(8), (1982) 29-36.

[6] S. Aoki, K. Kishimoto, M. Miyasaka, Analysis of potential and current-density distributions using a boundary element method, *Corrosion*, **44** (1988) 926-932.

[7] P. Miltiadou, C. Wrobel, Optimization of cathodic protection systems, using boundary elements and genetic algorithms, *Corrosion*, **58** (2002)912-921.

[8] D.P. Riemer, M.E. Orazem, Cathodic Protection of Multiple Pipelines with Coating Holidays, in: Proceedings of the NACE99 Topical Research Symposium: Cathodic Protection: Modeling and Experiment, M.E.
Orazem, Editor, NACE International, Houston, TX (1999) pp.65-81.

[9] D. Rabiot, F. Dalard, J.J. Rameau, J.P. Caire, S. Boyer, Study of sacrificial anode cathodic protection of buried tanks: Numerical modeling, *J. Appl. Electrochem.*,**29** (1999) 541-550.

[10] S. Aoki, K. Amaya, Optimization of cathodic protection system by BEM, *Eng. Anal. Bound. Elem.*,**19** (1997) 147-156.

[11] F. Brichau, J. Deconinck, A numerical-model for cathodic protection of buried pipes, *Corrosion*, **50** (1994) 39-49.

[12] M.E. Orazem, J.M. Esteban, K.J. Kennelley, R.M. Degerstadt, Mathematical models for cathodic protection of an underground pipeline with coating holidays. Part 1 -Theoretical development, *Corrosion*, **53** (1997) 264-272.

[13] K.J. Kennelley, L Bone, M.E. Orazem, Current and potential distribution on a coated pipeline with holidays.Part 1 - Model and experimental-verification, *Corrosion*, **49** (1993) 199-210.

[14] M.E. Orazem, K.J. Kennelley, L Bone, Current and potential distribution on a coated pipeline with holidays. Part 2 - Comparison of the effects of discrete and distributed holidays, *Corrosion*, **49** (1993) 211-219.

[15] R. Montoya, O. Rendon, J. Genesca, Mathematical simulation of a cathodic protection system by finite element method, Mater.Corros.,**56** (2005) 404-411.

[16] R. Montoya, W. Aperador, D.M. Bastidas, Influence of conductivity on cathodic protection of reinforced alkali-activated slag mortar using the finite element method, *Corrosion Sci.*, **51** (2009) 2857-2862.

[17] J.X. Jia, G.L. Song, A. Atrens, Experimental measurement and computer simulation of galvanic corrosion of magnesium coupled to steel, Adv. *Eng. Mater*., **9** (2007) 65-74.

[18] B. D. Reddy, Introductory functional analysis: With Applications to Boundary Values Problems and Finite Elements (Texts in Applied Mathematics, Vol. 27), Springer-Verlag, New York (1998).

[19] K. Rektorys, Variational Methods in Mathematics, Science and Engineering (Second Edn.), D. Reidel Publishing Co., Dordrecht (1980).

List of figures:

Figure 1. a) Schematic representation of a metallic circumference Γ_5 with a constant potential ϕ_0 immersed in an electrolyte Ω of conductivity *k*, which is limited by electrically insulated boundaries Γ_1, Γ_3, Γ_4 and another one with a non-nil current flow Γ_2. b) Graphic representation of the numerical solution of problem 2 found with FEM, considering $-k\frac{\partial\phi}{\partial n}=PC_{xjia}$A/m^{2}in$\Gamma_2$, ϕ_0 = −1.005V in Γ_5 and *k* = 4 mho/m.

Figure 2. a) Schematic representation of two metallic circumferences,Γ_5 and Γ_6,with a constant potential $\phi_0$immersed in an electrolyte $\Omega$of conductivity k which is limited by electrically insulated boundaries Γ_1, Γ_3, Γ_4 and another one with a non-nil current flow Γ_2. b) Graphic representations of numerical solution of the case shown in (a) found with FEM, considering $-k\frac{\partial\phi}{\partial n}=PC_{xjia}$A/m^2 in Γ_2, ϕ_0 = −1.005Vin$\Gamma_5$andΓ_6,and *k* = 4 mho/m. c) Graphic representations of numerical solution of the case shown in a) found with FEM, considering $-k\frac{\partial\phi}{\partial n}=PC_{xjia}$A/m^2 in Γ_2, ϕ_0 = −1.005VinΓ_5, *k* = 4 mho/m and using the RSPE in order to approximate the condition ϕ_0=−1.005VinΓ_6.

Figure 3.a) Schematic representation of three metallic circumferences Γ_5, Γ_6 and $\Gamma_7$with a constant potential ϕ_0 immersed in an electrolyte of conductivity k which is limited by electrically insulated boundaries Γ_1, Γ_3, Γ_4 and another one with a non-nil current flow Γ_2. b) Graphic representations of numerical solution of the case shown in a) found with FEM, considering $-k\frac{\partial\phi}{\partial n}=PC_{xjia}$A/m^2 in Γ_2, ϕ_0 = −1.005V in Γ_5, $\Gamma_6$and Γ_7 and *k* = 4 mho/m. c) Graphic representations of numerical solution of the case shown in (a) found with FEM, considering $-k\frac{\partial\phi}{\partial n}=PC_{xjia}$A/m^2 in Γ_2, ϕ_0 = −1.005V in Γ_2, ϕ_0 = −1.005V in Γ_5, *k* = 4 mho/m and using the RSPE in order to approximate the condition ϕ_0= −1.005V in Γ_6 and Γ_7.

Figure 4.Number of nodes used for solving the cases of one (I), two (II) and three (III) circular boundaries with coarse (A), medium (B) and fine (C) meshing respectively.

Figure 5. A) simplification of Figure 2 (a) with 4 paths, selected arbitrarily, where the potential profiles were obtained for problems 5 and 6 in order to be compared. I) potential profiles obtained in path I in A) using the red color line to represent the response of problem 5 and the black color representing the response of problem 6. It is clear that the red line is interrupted in the two anodes because problem 5 considers these ones as boundaries, but the black line is interrupted only in one anode due to problem 6 considers only one anode as boundary. II), III) and IV) show the potential profiles obtained in paths II), III) and IV), respectively, in A) using the red color line to represent the responses of problem 5 and the black color to represent the responses of problem 6.

Figure 6. a) Plot of the function $r\ exp\{(-s(x-x_0)^2-s(y-y_0)^2\}$ when r=12, x_0=y_0=0 and

D=1. b) It is clear that outside of the protuberance the function could be considered as zero.

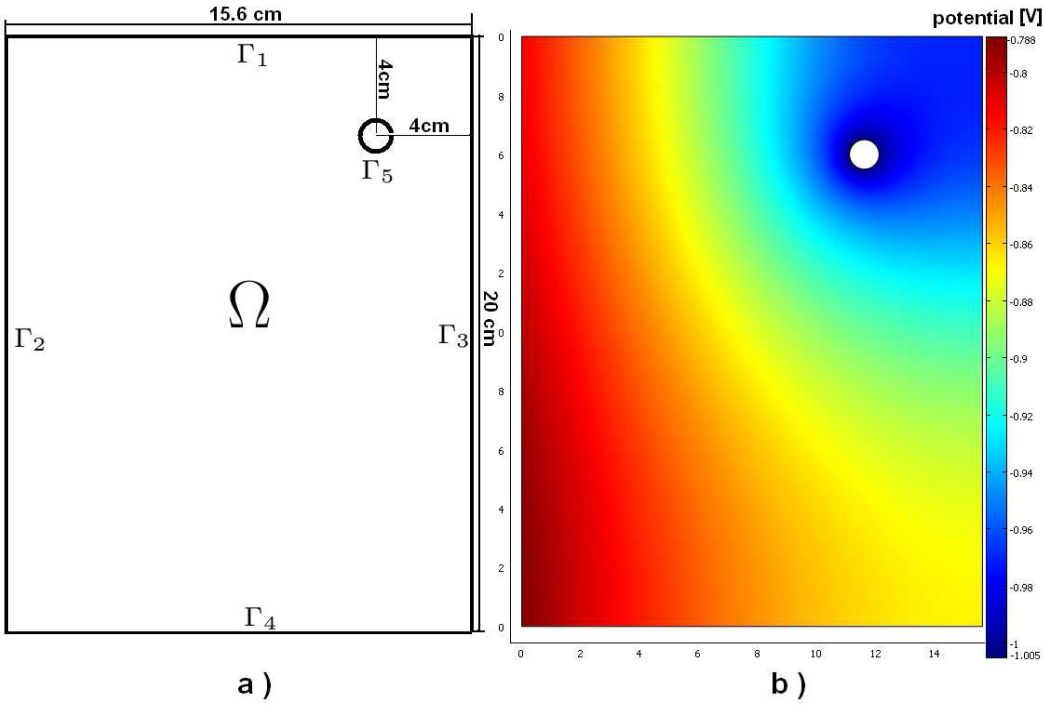

Figure 1.a) Schematic representation of a metallic circumference Γ_5 with a constant potential ϕ_0 immersed in an electrolyte Ω of conductivity k, which is limited by electrically insulated boundaries Γ_1, Γ_3, Γ_4 and another one with a non-nil current flow Γ_2. b) Graphic representation of the numerical solution of problem 2 found with FEM, considering $-k\frac{\partial \phi}{\partial n} = PC_{xjia}$ A/m^2 in Γ_2, $\phi_0 = -1.005$V in Γ_5 and $k = 4$ mho/m.

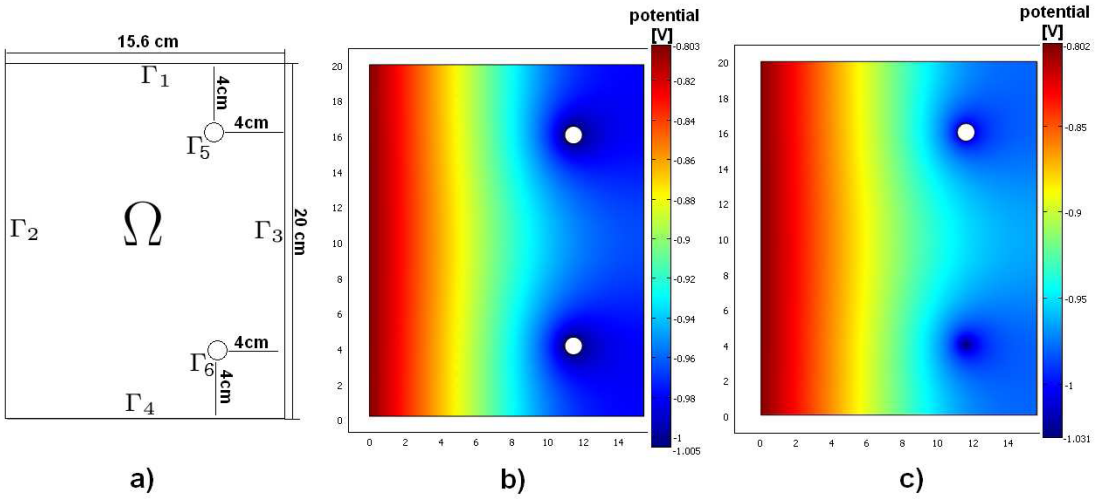

Figure 2. a) Schematic representation of two metallic circumferences Γ_5 and Γ_6 with a constant potential $\phi_0$immersed in an electrolyte Ω of conductivity k which is limited by electrically insulated boundaries Γ_1, Γ_3, Γ_4 and another one with a non-nil current flow Γ_2.b) Graphic representations of numerical solution of the case shown in a) found with FEM, considering $-k\frac{\partial\phi}{\partial n} = PC_{xjia}$A/m^2 in Γ_2, ϕ_0 = −1.005Vin$\Gamma_5$andΓ_6,and k = 4 mho/m.c) Graphic representations of numerical solution of the case shown in (a) found with FEM, considering $-k\frac{\partial\phi}{\partial n} = PC_{xjia}$A/m^2 in Γ_2, ϕ_0 = −1.005VinΓ_5, k = 4 mho/m and using the RSPE in order to approximate the condition ϕ_0=−1.005VinΓ_6.

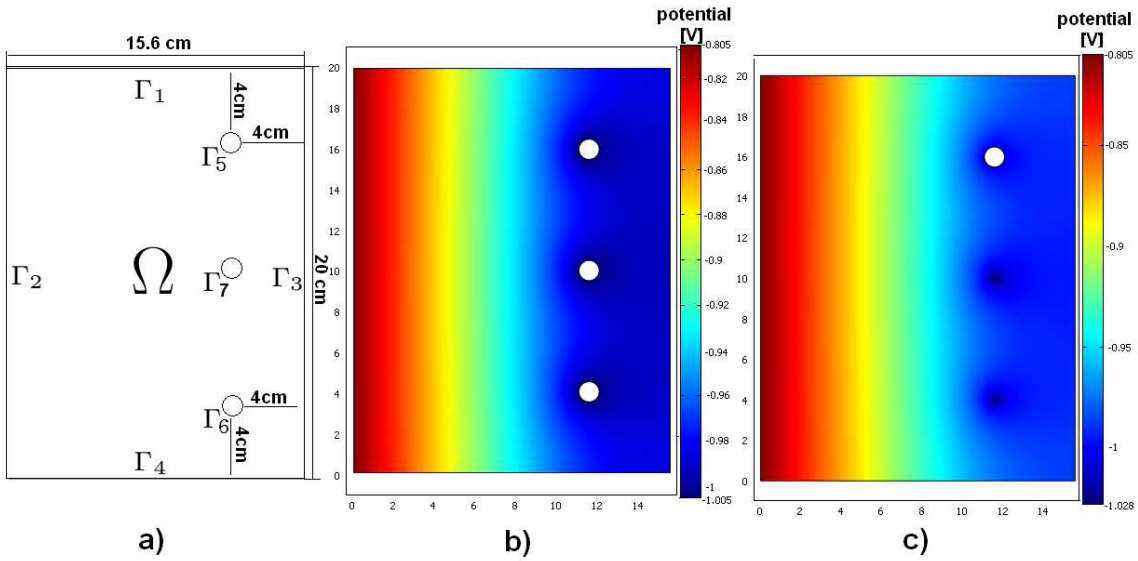

Figure 3.a) Schematic representation of three metallic circumferences Γ_5, Γ_6 and $\Gamma_7$with a constant potential ϕ_0 immersed in an electrolyte of conductivity k which is limited by electrically insulated boundaries Γ_1, Γ_3, Γ_4 and another one with a non-nil current flow Γ_2. b) Graphic representations of numerical solution of the case shown in a) found with FEM, considering $-k\frac{\partial\phi}{\partial n} = PC_{xjia}$A/m^2 in Γ_2, ϕ_0 = −1.005V in Γ_5, $\Gamma_6$and Γ_7 and k = 4 mho/m. c) Graphic representations of numerical solution of the case shown in (a) found with FEM, considering $-k\frac{\partial\phi}{\partial n} = PC_{xjia}$A/m^2 in Γ_2, ϕ_0 = −1.005V in Γ_2, ϕ_0 = −1.005V in Γ_5, k = 4 mho/m and using the RSPE in order to approximate the condition $\phi_0 = -1.005V$ in Γ_6 and Γ_7.

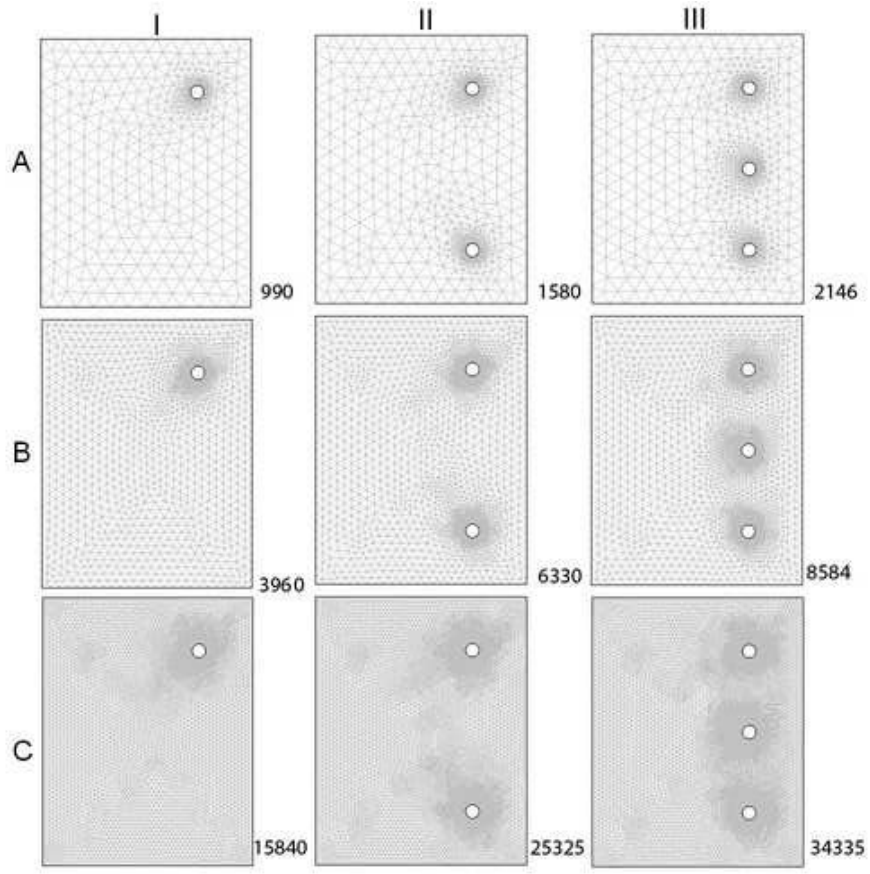

Figure 4. Number of nodes used for solving the cases of one (I), two (II) and three (III) circular boundaries with coarse (A), medium (B) and fine (C) meshing respectively.

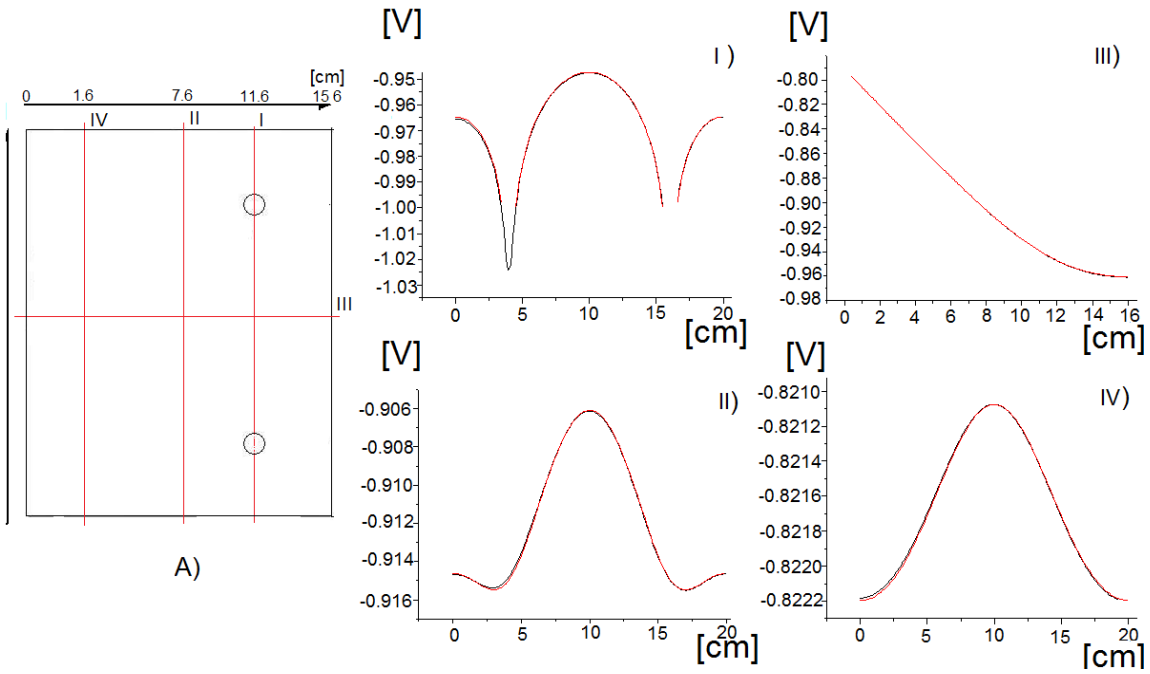

Figure 5. A) simplification of Figure 2 (a) with 4 paths, selected arbitrarily, where the potential profiles were obtained for problems 5 and 6 in order to be compared. I) potential profiles obtained in path I in A) using the red color line to represent the response of problem 5 and the black color representing the response of problem 6. It is clear that the red line is interrupted in the two anodes because problem 5 considers these ones as boundaries, but the black line is interrupted only in one anode due to problem 6 considers only one anode as boundary. II), III) and IV) show the potential profiles obtained in paths II), III) and IV), respectively, in A) using the red color line to represent the responses of problem 5 and the black color to represent the responses of problem 6.

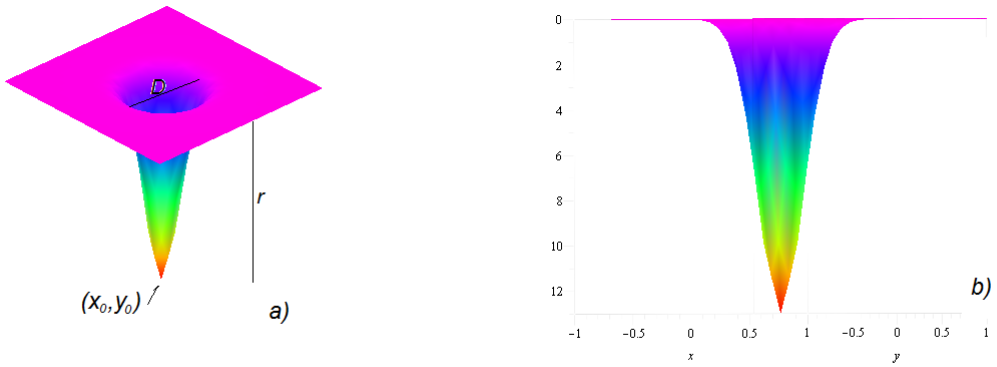

Figure 6. a) Plot of the function $r\ exp\{(-s(x-x_0)^2 - s(y-y_0)^2\}$ when r=12, x_0=y_0=0 and D=1. b) It is clear that outside of the protuberance the function could be considered as zero.